

Review of the Major and Minor Salivary Glands, Part 1: Anatomy, Infectious, and Inflammatory Processes

Alexander T Kessler, Alok A Bhatt

Department of Imaging Sciences, University of Rochester Medical Center, Rochester, New York, USA



Received : 16-06-2018
Accepted : 06-10-2018
Published : 15-11-2018

ABSTRACT

The major and minor salivary glands of the head and neck are important structures that contribute to many of the normal physiologic processes of the aerodigestive tract. The major salivary glands are routinely included within the field of view of standard neuroimaging, and although easily identifiable, salivary pathology is relatively rare and often easy to overlook. Knowledge of the normal and abnormal imaging appearance of the salivary glands is critical for forming useful differential diagnoses, as well as initiating proper clinical workup for what are often incidental findings. The purpose of this review is to provide a succinct image-rich article illustrating relevant anatomy and pathology of the salivary glands via an extensive review of the primary literature. In Part 1, we review anatomy as well as provide an in-depth discussion of the various infectious and inflammatory processes that can affect the salivary glands.

KEYWORDS: *Mumps virus, salivary gland calculi, salivary glands, sialadenitis, Sjogren's syndrome*

INTRODUCTION

The salivary glands constitute a diverse group of anatomic structures that can give rise to a wide variety of unique pathology. The major salivary glands are easily identified on routine imaging and contribute to many of the important deep neck spaces of the suprahyoid neck. The minor salivary glands are poorly visualized on routine imaging, but can also give rise to salivary pathology anywhere along the aerodigestive tract. After an extensive review of the radiology, otolaryngology, and pathology literature, we present a comprehensive discussion of salivary gland anatomy, as well as illustrate the broad range of nonneoplastic disease that can be visualized in the salivary glands.

ANATOMY OF THE MAJOR SALIVARY GLANDS

The parotid gland is the largest of the three major salivary glands. It is superficial in location and enclosed by the superficial layer of the deep cervical fascia where it forms the aptly named parotid space. The parotid space is located posterolateral to the masticator space, lateral to the parapharyngeal space, and anterolateral to the carotid space [Figure 1]. Aside from

the gland itself, the parotid space is also comprised of the facial nerve (CN VII), auriculotemporal branches of the mandibular division of the trigeminal nerve (CN V3), intraparotid lymph nodes, the external carotid artery, and the retromandibular vein.^[1-3] Although not a true fascial plane, the intraparotid facial nerve separates the parotid gland into superficial and deep portions, an important distinction to make when describing a lesion's location before excision. The branches of the facial nerve are not always visualized on routine imaging, and therefore, the retromandibular vein or stylomandibular tunnel is commonly used as surrogate landmark for its location. It is important to note that late encapsulation of the parotid gland during embryogenesis results in the presence of lymphoid tissue within the parotid gland. This is a unique feature among the salivary glands and allows the parotid gland to develop lymphoid pathology.

Address for correspondence: Dr. Alexander T Kessler, 601 Elmwood Avenue, Box 648, Rochester, New York 14642, USA. E-mail: atkessler8@gmail.com

This is an open access journal, and articles are distributed under the terms of the Creative Commons Attribution-NonCommercial-ShareAlike 4.0 License, which allows others to remix, tweak, and build upon the work non-commercially, as long as appropriate credit is given and the new creations are licensed under the identical terms.

For reprints contact: reprints@medknow.com

How to cite this article: Kessler AT, Bhatt AA. Review of the Major and Minor Salivary Glands, Part 1: Anatomy, Infectious, and Inflammatory Processes. J Clin Imaging Sci 2018;8:47. Available FREE in open access from: <http://www.clinicalimagingscience.org/text.asp?2018/8/1/47/245527>

Access this article online	
Quick Response Code: 	Website: www.clinicalimagingscience.org
	DOI: 10.4103/jcis.JCIS_45_18

The parotid (Stensen's) duct arises from the anterior border of the parotid gland and courses ventrally along the superficial surface of the masseter muscle. It then makes a gentle turn medially where it pierces the buccinator muscle and opens opposite the 2nd maxillary molar [Figure 2]. It is important to note that 21%–61% of individuals have accessory parotid tissue extending ventrally over the masseter muscle, often with a secondary duct that drains directly into the main parotid duct.

The submandibular gland is the second largest of the three major salivary glands. It is located deep to the angle of the mandible and straddles both the submandibular and sublingual spaces. The submandibular space is enveloped in the superficial layer of the deep cervical fascia and is bounded by the mandible anteriorly, anterior belly of the digastric muscle posteromedially, mylohyoid muscle anterosuperiorly, and hyoid bone

inferiorly [Figure 3]. Although not a true fascial plane, a line drawn through the submandibular gland at the level of the posterior margin of the mylohyoid muscle can be used to separate the submandibular (superficial) portion of the submandibular gland from the sublingual (deep) portion of the submandibular gland. Aside from the superficial portion of the submandibular gland, the submandibular space is also comprised of level Ib lymph nodes, the facial artery/vein, and branches of the hypoglossal nerve.^[1-4]

The submandibular (Wharton's) duct arises from the anterior border of the submandibular gland and courses through the sublingual space in between the mylohyoid muscle/sublingual gland laterally and hyoglossus/genioglossus muscles medially [Figure 3]. It then continues anteriorly and superiorly where it ultimately drains into the sublingual caruncle along the side of the frenulum in the floor of the mouth.

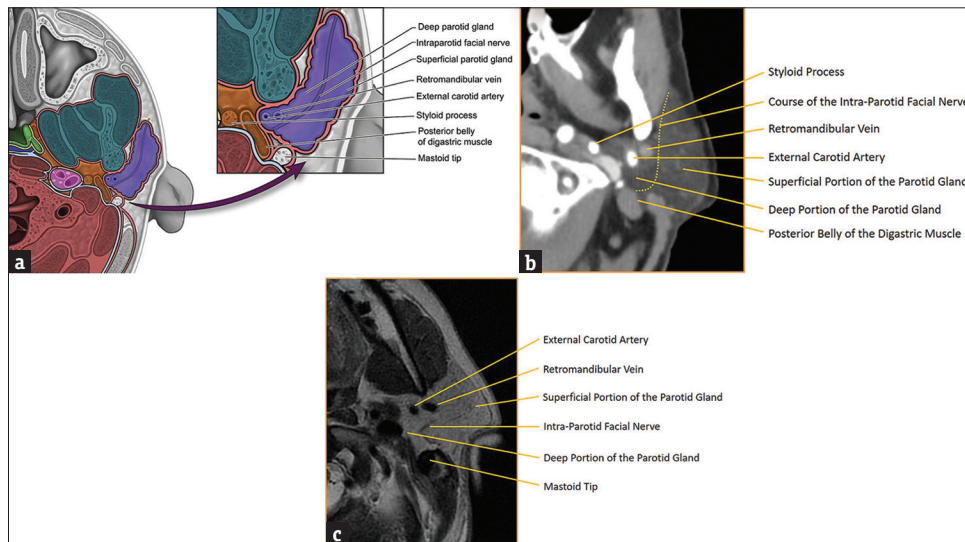


Figure 1: Parotid space anatomy. (a) Illustration of parotid space anatomy with key landmarks labeled. (b) Axial computed tomography of parotid space anatomy with key landmarks labeled. (c) Axial T2-weighted magnetic resonance image of parotid space anatomy with key landmarks labeled.

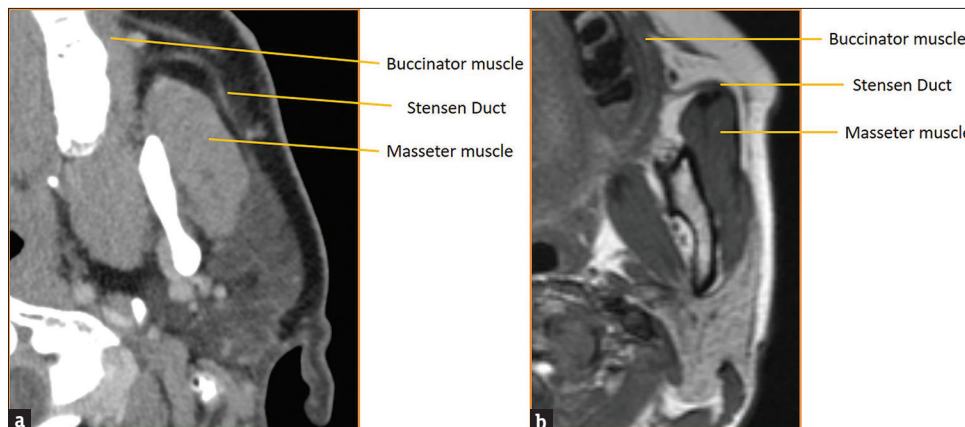


Figure 2: Parotid (Stensen) duct anatomy. (a) Axial computed tomography of parotid duct anatomy with key landmarks labeled. (b) Axial T2-weighted magnetic resonance image of parotid duct anatomy with key landmarks labeled.

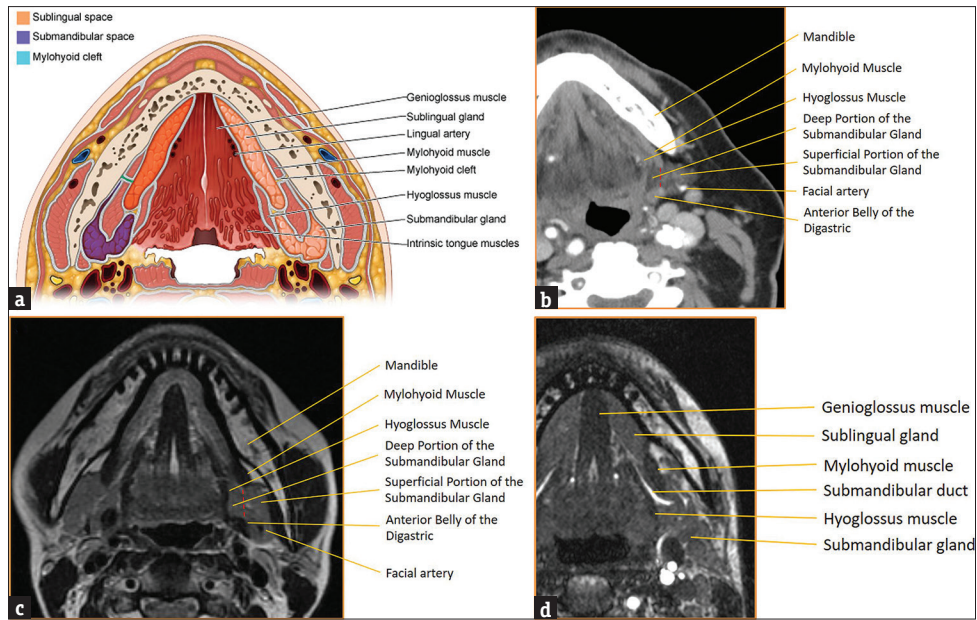


Figure 3: Submandibular space anatomy. (a) Illustration of submandibular and sublingual space anatomy with key landmarks labeled. (b) Axial computed tomography of submandibular space anatomy with key landmarks labeled. (c) Axial T2-weighted magnetic resonance image of submandibular space anatomy with key landmarks labeled. (d) Axial T2-weighted magnetic resonance image of submandibular duct anatomy with key landmarks labeled.

The sublingual gland is the smallest of the three major salivary glands. It is located deep to the body of the mandible and located with the sublingual space. The sublingual space is enveloped in the superficial layer of the deep cervical fascia and is bounded by the mandible anteriorly, genioglossus/geniohyoid muscles medially, mylohyoid muscle posterolaterally, and intrinsic muscles of the tongue superiorly [Figure 4]. Aside from the sublingual gland, the sublingual space is also comprised of the deep portion of the submandibular gland, the submandibular duct, the lingual artery/vein, and the lingual branch of the mandibular division of the trigeminal nerve (CN V3).^[1-4] The sublingual gland itself is composed of a major sublingual gland and 8–30 small minor sublingual glands. The sublingual duct (Bartholin’s duct) drains the major sublingual gland into Wharton’s duct while multiple tiny ducts of Rivinus drain the minor sublingual glands into the floor of the mouth.

The mylohyoid sling acts as the major anatomic separator between the submandibular space inferolaterally from the sublingual space superomedially. However, it is important to note that these two spaces freely communicate via a gap along the posterior margin of the mylohyoid muscle [Figure 5]. Up to 77% of individuals have a cleft (boutonniere) in the mylohyoid muscle allowing for a 2nd pathway for spread of disease between the two spaces. This cleft is often filled with fat or a herniated portion of the sublingual gland [Figure 5].^[5,6]

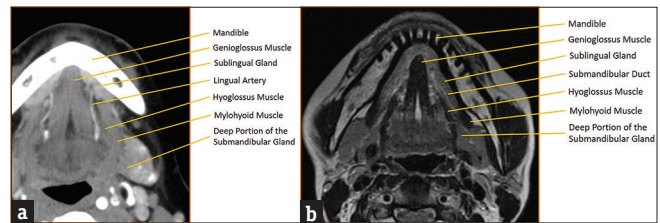


Figure 4: Sublingual space anatomy. (a) Axial computed tomography of sublingual space anatomy with key landmarks labeled. (b) Axial T2-weighted magnetic resonance imaging image of sublingual space anatomy with key landmarks labeled.

ANATOMY OF THE MINOR SALIVARY GLANDS

Minor salivary gland tissue is comprised of 800-1000 small salivary glands dispersed throughout the submucosa of the sinonasal cavity, oral cavity, pharynx, larynx, trachea, lungs, and middle ear cavity. Although minor salivary gland tissue can be found anywhere along the aerodigestive tract, it is most concentrated along the buccal mucosa, labial mucosa, lingual mucosa, soft/hard palate, and floor of mouth [Figure 6].^[1,2] Minor salivary gland tissue is not normally seen on conventional imaging, but can become apparent when replaced by tumor or benign processes, most commonly mucus retention cysts.^[7]

INFECTIOUS/INFLAMMATORY PROCESSES OF THE SALIVARY GLANDS

Sialolithiasis

Sialolithiasis, or calculus disease, is the most common benign process to affect the salivary glands, with a

reported prevalence of 1.2%.^[8] The pathogenesis of sialolithiasis is highly debated, but thought to be due to stagnation of saliva that is high in calcium. Risk factors include dehydration, smoking, and various medications (most commonly anticholinergics and diuretics). The majority of calculi are found within the submandibular gland (80%–92%), likely due to the fact that the submandibular gland produces highly viscous saliva that needs to travel upward against gravity as it traverses Wharton’s duct.^[9,10] The remaining calculi are found in the parotid gland (6%–20%) and sublingual/minor salivary glands (1%–2%).

Patients with sialolithiasis typically present with painful salivary glands, exacerbated by eating foods that precipitate saliva production. Unenhanced CT has replaced radiography as the first-line imaging test to workup sialolithiasis, mostly due to its improved sensitivity for detecting calcifications, intraglandular masses, and adjacent inflammatory standing [Figure 7]. If no calculus is found and there

is a high suspicion for a nonradiopaque calculus, conventional sialography can be performed [Figure 8]. Alternatively, many institutions have now adopted magnetic resonance (MR) sialography (single-shot fast spin echo heavily T2-weighted sequence similar to an MR cholangiopancreatography) as a means to identify these previously “occult” calculi. Sialography (conventional or MR imaging) provides the additional benefit of a global assessment of the salivary gland ductal system, allowing for the identification of strictures and changes related to chronic inflammation.

Sialadenitis

Sialadenitis is a general term used to denote an infectious or inflammatory process of the salivary glands. This is not to be confused with sialosis, which refers to bilateral symmetric painless enlargement of the salivary glands often due to diabetes, alcohol, obesity, or medications. Sialadenitis can be due to a variety of causes including viral, bacterial, fungal, parasitic,

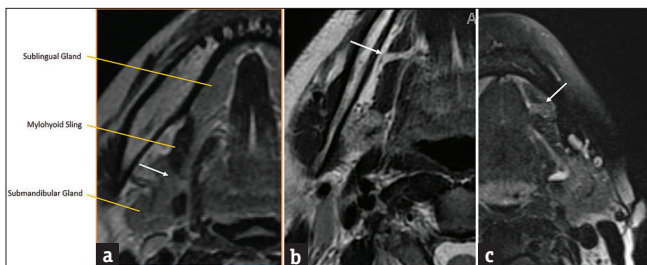


Figure 5: Mylohyoid sling/cleft. (a) Axial T2-weighted magnetic resonance image demonstrates the mylohyoid sling with normal free communication posteriorly between submandibular and sublingual spaces (white arrow). (b) Axial T2-weighted magnetic resonance image demonstrates a fat-filled mylohyoid cleft (white arrow). (c) Axial T2-weighted magnetic resonance imaging image demonstrates a mylohyoid cleft containing herniated sublingual gland (white arrow).

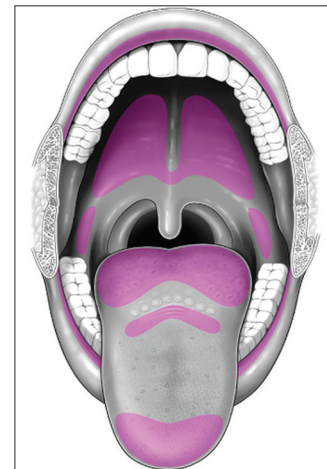


Figure 6: Minor salivary gland distribution in the oral cavity (purple).

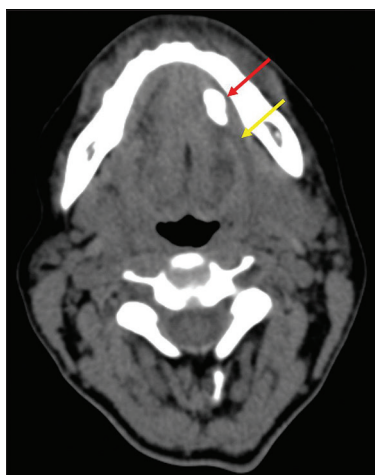


Figure 7: Sialolithiasis – computed tomography. Axial computed tomography image demonstrates a submandibular duct sialolith (red arrow) with dilated proximal duct (yellow arrow).

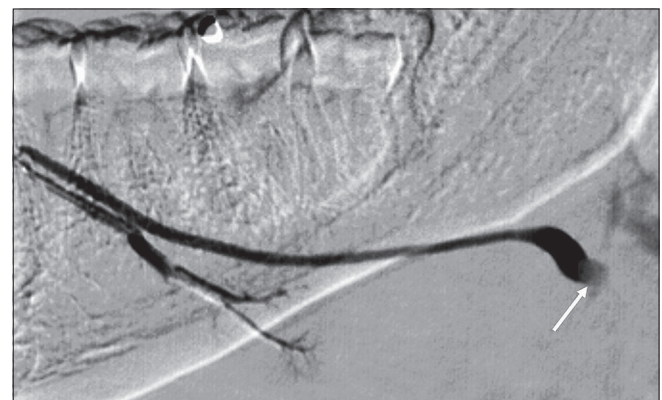


Figure 8: Sialolithiasis – Sialography. Right submandibular duct sialogram in a 36-year-old female demonstrates a filling defect (white arrow) at the expected location of the hilum of the submandibular gland, compatible with a calculus.

immunologically mediated disease, and granulomatous processes. Of these, infection is the most common cause of sialadenitis, typically due to viral or polymicrobial bacterial pathogens.

Infectious sialadenitis

Worldwide, viral sialadenitis is most commonly due to mumps virus; however, many other viruses including parainfluenza, influenza, coxsackie, Epstein-Barr virus, herpes simplex virus, and HIV have also been implicated. In the United States, aggressive vaccination has significantly decreased the prevalence of mumps sialadenitis, with approximately 300 cases reported annually.^[11] That being said, mumps sialadenitis has been well described in the literature and provides a framework for understanding the pathophysiology of most types of viral sialadenitis. Clinically, mumps sialadenitis begins with a prodromal period followed by acute bilateral salivary gland swelling typically affecting the parotid glands. However, it is important to note that up to 30% of mumps infections can be asymptomatic or may present as vague upper respiratory symptoms without salivary gland swelling. On imaging, classic findings include bilateral enlargement of the salivary glands, fat stranding, and thickening of the superficial cervical fascia and platysma muscles [Figure 9].^[12,13] Although bilateral involvement is seen in up to 75% of patients, a small minority of patients may present with only unilateral involvement. In these cases, clinical confirmation through the detection of anti-mumps immunoglobulin-M (IgM) antibodies, IgG titer, or viral polymerase chain reaction is required.

HIV patients are an interesting demographic with regard to infectious sialadenitis. Although sialadenitis

in HIV patients is most commonly due to the same viral/bacterial pathogens as non-HIV patients, they can develop a separate entity referred to as HIV-associated salivary gland disease. This is characterized by progressive, painless swelling of the bilateral salivary glands due to the formation of benign lymphoepithelial cysts (BLECs).^[14] Although rare in patients receiving highly active antiretroviral therapy, this entity can be seen in HIV patients with poorly controlled CD4 counts [Figure 10].

Unlike viral sialadenitis, bacterial sialadenitis presents with acute unilateral salivary gland swelling without a preceding prodromal period. The most common bacterial pathogens are *Staphylococcus aureus* and anaerobes; however, Gram-negative organisms predominate in the hospitalized subset of patients.^[15] On imaging, classic findings include unilateral enlargement of a salivary gland, fat stranding, and thickening of the superficial cervical fascia and platysma muscle [Figure 11]. In these patients, it is important to look for additional findings that suggest that the sialadenitis will not resolve with conservative therapy alone. These include the presence of a drainable abscess or a large calculus (>10 mm) that will have difficulty passing on its own without surgical retrieval [Figure 12].^[1] Many predisposing risk factors for infectious sialadenitis have been identified and are generally broken down into two categories: modifiable and nonmodifiable. Modifiable risk factors include dehydration, malnutrition, sialolithiasis, recent surgery, and medications (anticholinergics, diuretics, and chemotherapy). Nonmodifiable risk factors include age (elderly), anorexia nervosa, cystic fibrosis, diabetes, HIV/AIDS, hepatic/renal failure, and prior radiation.

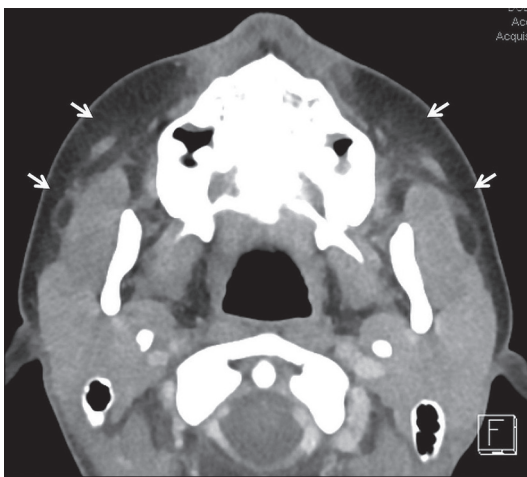


Figure 9: Viral Sialadenitis. Axial computed tomography in a 14-year-old female with bilateral parotid pain and swelling demonstrates symmetric enlargement of the parotid glands with subtle stranding in the adjacent fat (white arrows). Blood work was positive for parainfluenza virus.



Figure 10: HIV Sialadenitis. A 44-year-old female with HIV not on highly active antiretroviral therapy (CD4 109) presenting with 1 month of progressive painless bilateral parotid swelling. Axial computed tomography demonstrates heterogeneous attenuation throughout the parotid glands with prominent cystic lesions (white arrows), benign lymphoepithelial cysts.

Inflammatory sialadenitis

Autoimmune sialadenitis refers to a group of noninfectious disorders that result in chronic inflammation and fibrosis of the salivary glands. Two of the more common autoimmune processes include Sjogren's syndrome and sarcoidosis. Sjogren's sialadenitis is a female predominant disorder (>90%) most commonly seen in the postmenopausal age group (50–70 years of age). However, there is a juvenile subtype seen in men aged <20 years that typically resolves at puberty. Sjogren's sialadenitis is classified into two types. Sjogren's type 1 disease (Mikulicz's disease or "sicca syndrome without a connective tissue disorder") refers to autoimmune inflammation of the salivary glands without a systemic collagen vascular disorder. These patients present with xerostomia and have been recently incorporated into the IgG4 spectrum of disease. Sjogren's type 2 disease refers to autoimmune inflammation of the salivary glands with a systemic autoimmune process (rheumatoid arthritis > systemic lupus erythematosus > scleroderma). On imaging, early changes of Sjogren's sialadenitis include enlarged parotid glands, small cysts, and mild fatty replacement [Figure 13]. As the disease process becomes chronic, imaging findings shift toward parotid atrophy, larger areas of fatty replacement, parenchymal calcifications, solid masses of lymph node aggregates, and either large areas of cystic destruction or multiple lymphoepithelial cysts (similar to HIV BLECs).^[16] On sialography, chronic Sjogren's sialadenitis demonstrates alternating ductal stenosis and dilatation ("string of beads" sign) [Figure 14]. It is important to note that patients with Sjogren's sialadenitis carry a 14-fold increased risk of developing non-Hodgkin's lymphoma [Figure 15].^[17]

Sarcoid sialadenitis refers to chronic inflammation of the salivary glands in patients with sarcoidosis. It is seen in 10%–30% of patients with sarcoidosis and patients typically present with painless bilateral parotid swelling. Imaging may show nonspecific intraparotid masses corresponding to granulomatous lymph node aggregates. Alternatively, imaging may show symmetric enlargement and hypervascularity of the parotid and lacrimal glands [Figure 16], producing the classic "Panda sign" on gallium-67 scans.^[18]

Chronic sclerosing sialadenitis, also known as Kuttner's tumor, refers to chronic enlargement of the salivary glands due to an immune-mediated infiltration of lymphoplasmacytic cells. Although quite rare, this disease entity has a peak incidence in the 6th–8th decades, with a slight male predilection.^[19] The overwhelming

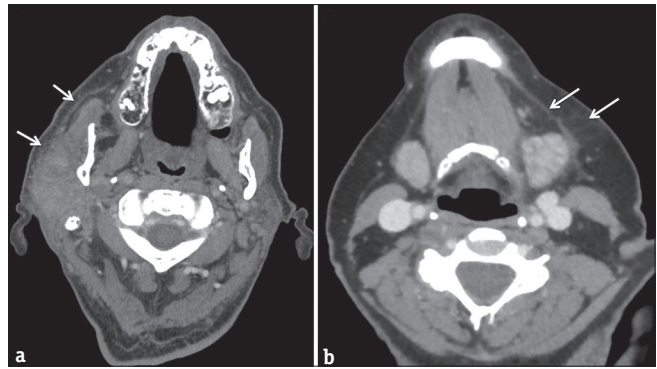


Figure 11: Bacterial sialadenitis. (a) Axial computed tomography in a 70-year-old male with acute right parotid swelling and purulent drainage. (b) Axial computed tomography in a 69-year-old female with acute left submandibular swelling. Both cases demonstrate asymmetric enlargement of a salivary gland with thickening of the adjacent platysma muscle and stranding in the subcutaneous fat (white arrows). Both cases resolved clinically after antibiotics.

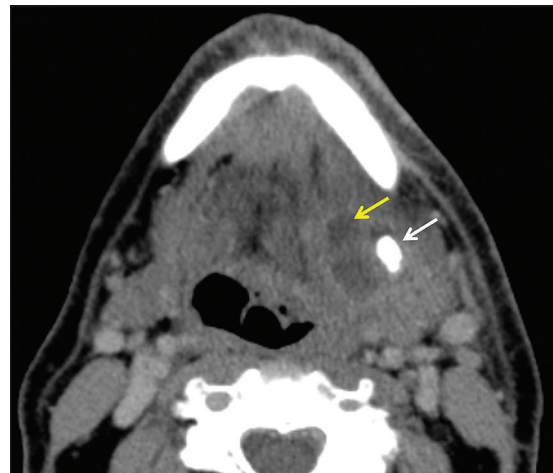


Figure 12: Salivary gland abscess. A 69-year-old male presents with left submandibular swelling and purulent drainage. Axial computed tomography demonstrates asymmetric enlargement of the left submandibular gland with thickening of the adjacent platysma and fat stranding. A large 1.2 cm sialolith (white arrow) and 2 cm abscess (yellow arrow) are also present. The patient ultimately required surgical excision of the submandibular gland and abscess drainage.

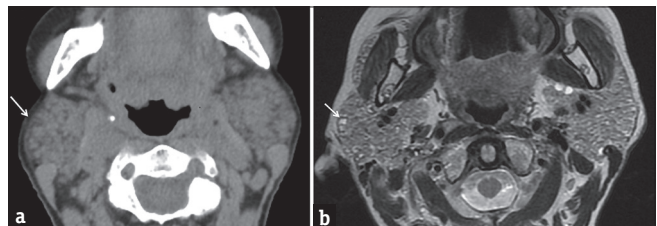


Figure 13: Early Sjogren's syndrome. Axial computed tomography (a) and axial T2-weighted magnetic resonance image (b) demonstrate enlarged parotid glands with areas of cystic changes (white arrows).

majority of cases involve the submandibular glands, and recent literature has demonstrated a strong association with IgG4-related disease. In fact, a recent case series by Geyer et al., demonstrated IgG4 plasma cell infiltrates in 92% of patients with chronic sclerosing

sialadenitis.^[20] On imaging, the involved gland is enlarged and demonstrates homogeneous enhancement, often mimicking a malignant neoplasm. Advanced MR imaging with diffusion-weighted imaging and dynamic contrast-enhanced (DCE) perfusion imaging is also nonspecific, although low apparent diffusion coefficient (ADC) signal and rapid washout on DCE time curves have been described.^[21] Although biopsy is often needed to confirm the diagnosis, knowledge of this entity can help avoid misdiagnosis, as well as initiate the workup for other sites of IgG4-related disease.

Postradiation sialadenitis

Radiation-induced sialadenitis is frequently seen in patients who receive radiation treatment for oropharyngeal cancer. The first clinical signs of sialadenitis manifest as decreased saliva flow and have been reported to occur with radiation dose thresholds as low as 15 Gy.^[22] The classic imaging findings of radiation-induced sialadenitis include hyperenhancement of the salivary glands that progresses to atrophy over time [Figure 17]. This hyperenhancement occurs with

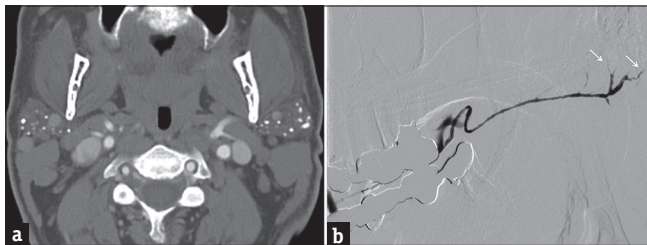


Figure 14: Chronic Sjogren's syndrome. (a) Axial computed tomography demonstrates atrophic parotid glands with multiple parenchymal calcifications. (b) Sialogram of the left submandibular duct demonstrates multifocal areas of narrowing/irregularity through the main duct with pruning of the intraglandular ducts (white arrows).

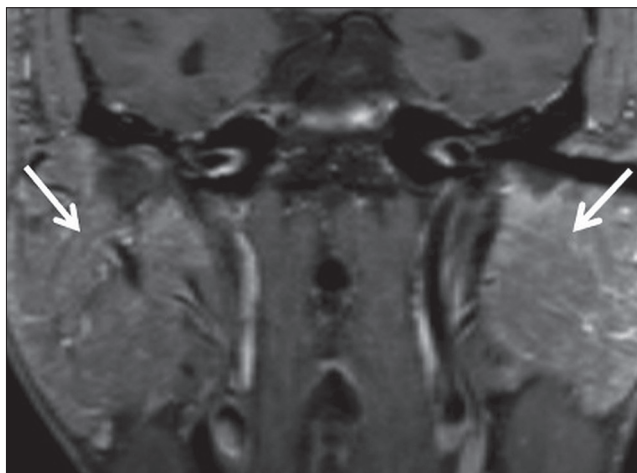


Figure 16: Sarcoid sialadenitis. A 51-year-old male with a history of pulmonary sarcoidosis presents with bilateral parotid swelling. Coronal T1 FS + C images demonstrate marked enlargement and hyperenhancement of the bilateral parotid glands (white arrows), presumably reflecting sarcoid sialadenitis.

doses >45 Gy and is thought to represent contrast expanding the extracellular space that was once occupied by acinar cells lost from radiation.^[23] Over time, chronic scarring/fibrosis leads to volume loss and MR imaging typically demonstrates low-to-intermediate signal intensity on all sequences.^[24]

CONCLUSION

A variety of disease processes can occur within salivary gland tissue, and it is important to be familiar with their imaging findings. However, the rarity in which salivary pathology is encountered often leads to improper characterization or misidentification. By illustrating the normal anatomy and common infectious/inflammatory processes within the major and minor salivary glands across multiple imaging modalities, we hoped to enhance

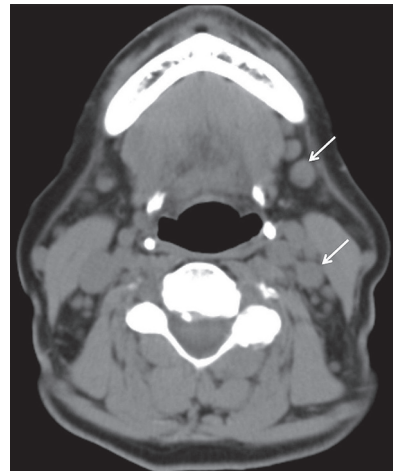


Figure 15: Sjogren's syndrome with lymphoma. A 76-year-old female with a history of Sjogren's syndrome with bilateral palpable cervical lymph nodes. Axial computed tomography demonstrates multiple mildly enlarged level Ib and IIb lymph nodes (white arrows). Biopsy proved non-Hodgkin lymphoma.

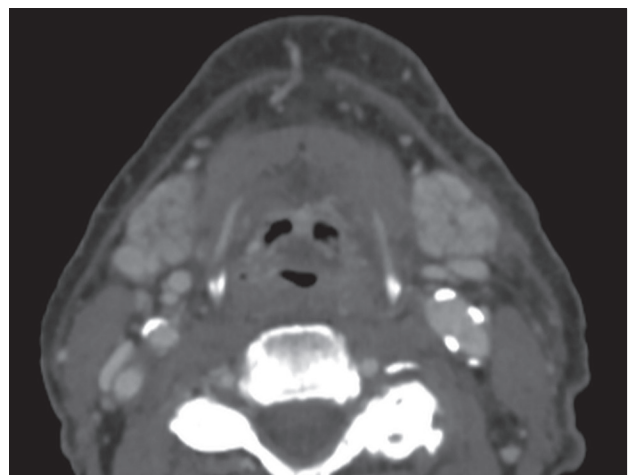


Figure 17: Radiation-induced sialadenitis. Axial computed tomography demonstrates hyperenhancement of the bilateral submandibular glands in a patient recently treated with external beam radiation for oropharyngeal cancer.

the imager's search pattern and improve diagnostic accuracy.

Financial support and sponsorship

Nil.

Conflicts of interest

There are no conflicts of interest.

REFERENCES

- Som PM, Brandwin-Gensler MS. Anatomy and pathology of the salivary glands. In: Som PM, Curtin HD, editors. *Head and Neck Imaging*. 5th ed. St. Louis: Mosby; 2011. p. 2449-602.
- Grossman RI, Yousem DM, editors. *Extramucosal diseases of the head and neck*. In: *Neuroradiology: The Requisites*. 3rd ed. St. Louis: Mosby; 2010. p. 476-514.
- Rastogi R, Bhargava S, Mallarajapatna GJ, Singh SK. Pictorial essay: Salivary gland imaging. *Indian J Radiol Imaging* 2012;22:325-33.
- La'porte SJ, Juttla JK, Lingam RK. Imaging the floor of the mouth and the sublingual space. *Radiographics* 2011;31:1215-30.
- Otonari-Yamamoto M, Nakajima K, Tsuji Y, Otonari T, Curtin HD, Okano T, et al. Imaging of the mylohyoid muscle: Separation of submandibular and sublingual spaces. *AJR Am J Roentgenol* 2010;194:W431-8.
- White DK, Davidson HC, Harnsberger HR, Haller J, Kanya A. Accessory salivary tissue in the mylohyoid boutonnière: A clinical and radiologic pseudolesion of the oral cavity. *AJNR Am J Neuroradiol* 2001;22:406-12.
- Senthikumar B, Nazargi Mahabob M. Mucocele: An unusual presentation of the minor salivary gland lesion. *J Pharm Bioallied Sci* 2012;4:180-2.
- Harrison JD. Causes, natural history, and incidence of salivary stones and obstructions. *Otolaryngol Clin North Am* 2009;42:927-47.
- Yousem DM, Kraut MA, Chalian AA. Major salivary gland imaging. *Radiology* 2000;216:19-29.
- Mandel L. Salivary gland disorders. *Med Clin North Am* 2014;98:1407-49.
- Barskey AE, Juieng P, Whitaker BL, Erdman DD, Oberste MS, Chern SW, et al. Viruses detected among sporadic cases of parotitis, United States, 2009-2011. *J Infect Dis* 2013;208:1979-86.
- Brook I. The bacteriology of salivary gland infections. *Oral Maxillofac Surg Clin North Am* 2009;21:269-74.
- Zenk J, Iro H, Klintworth N, Lell M. Diagnostic imaging in sialadenitis. *Oral Maxillofac Surg Clin North Am* 2009;21:275-92.
- Shanti RM, Aziz SR. HIV-associated salivary gland disease. *Oral Maxillofac Surg Clin North Am* 2009;21:339-43.
- Al-Dajani N, Wootton SH. Cervical lymphadenitis, suppurative parotitis, thyroiditis, and infected cysts. *Infect Dis Clin North Am* 2007;21:523-41, viii.
- Gomes Pde S, Juodzbaly G, Fernandes MH, Guobis Z. Diagnostic approaches to Sjögren's syndrome: A Literature review and own clinical experience. *J Oral Maxillofac Res* 2012;3:e3.
- Liang Y, Yang Z, Qin B, Zhong R. Primary Sjogren's syndrome and malignancy risk: A systematic review and meta-analysis. *Ann Rheum Dis* 2014;73:1151-6.
- Kurdziel KA. The panda sign. *Radiology* 2000;215:884-5.
- Wei TW, Lien CF, Hsu TY, He HL. Chronic sclerosing sialadenitis of the submandibular gland: An entity of igG4-related sclerosing disease. *Int J Clin Exp Pathol* 2015;8:8628-31.
- Geyer JT, Ferry JA, Harris NL, Stone JH, Zukerberg LR, Lauwers GY, et al. Chronic sclerosing sialadenitis (Küttner tumor) is an igG4-associated disease. *Am J Surg Pathol* 2010;34:202-10.
- Abu A, Motoori K, Yamamoto S, Hanazawa T, Nagai Y, Kaneoya K, et al. MRI of chronic sclerosing sialoadenitis. *Br J Radiol* 2008;81:531-6.
- Cheng SC, Wu VW, Kwong DL, Ying MT. Assessment of post-radiotherapy salivary glands. *Br J Radiol* 2011;84:393-402.
- Bronstein AD, Nyberg DA, Schwartz AN, Shuman WP, Griffin BR. Increased salivary gland density on contrast-enhanced CT after head and neck radiation. *AJR Am J Roentgenol* 1987;149:1259-63.
- Houweling AC, van den Berg CA, Roesink JM, Terhaard CH, Raaijmakers CP. Magnetic resonance imaging at 3.0T for submandibular gland sparing radiotherapy. *Radiother Oncol* 2010;97:239-43.